ISSN 2083-1587; e-ISSN 2449-5999
2025,Vol. 29,No.1, pp. 347-360
Agricultural Engineering
www://agriceng.org
DOI: 10.2478/agriceng-2025-0020

DYNAMIC SIMULATION AND EXPERIMENTAL VALIDATION OF HYDRAULIC PERFORMANCE FOR A VALVE-REGULATED PROPORTIONAL FERTIGATOR

Zakaria Issaka[a*]

[a] Department of Agricultural Engineering, Tamale Technical University, P. O. Box 3 E/R, Northern Region, Ghana, e-mail: issakazak@gmail.com, ORCID 0000-0002-8629-0656

Corresponding author: e-mail: issakazak@gmail.com

ARTICLE INFO

Article history:
Received: April 2025
Received in the revised form: September 2025
Accepted: November 2025

Keywords:
Valve-regulated proportional fertigator;
three-way flow control valve;
fertilizer ratio;
dynamic mesh;
driving force

ABSTRACT

With the sustainable development of precision agriculture, the valve regulated proportional fertigator has attracted research attention due to its high efficiency combined with low cost and incidence of damage. In order to investigate the hydraulic performance of the fertigator, the internal flow, force and motion of the piston were analysed by means of dynamic simulation and experimental validation. Results show that the inlet flow of fertilizer first increased and then decreased with the increase of the three-way valve angle under the same pressure conditions. The area with the highest flow velocity of 13 m/s in the fertigator concentrates on the inlet one-way valve and three-way valve part, while the fertilizer extraction part and the outlet part were in the low flow velocity area. The movement frequency increased with the increase of the three-way valve angle, except the middle part that showed variations in the wave change. With the increase of the inlet pressure, the variations in the three-way valve angles were also increased. At the initial stage of piston motion, the driving force was much greater than the resistance, and the driving force and the resistance fluctuated from the initial maximum to the same stable value. The resultant force of the piston fluctuates from the initial maximum driving force of 242 N to 0 N, and then the piston accelerates from 0 N to the minimum driving force of 8.5 N. When the resultant force was reduced, the acceleration also decreased. However, when the acceleration was reduced to zero (0), the piston started to move uniformly, which is useful for achieving consistency in the spread of fertilizer application in the artificially drained catchment. The maximum relative error between simulation and experiment was 15%. However, there was no difference in the overall trend, so we can draw a reasonable and accurate conclusion of the simulation. The study could be useful for achieving uniformity in the spread of fertilizer application in the artificially drained catchment.

Introduction

An indispensable part of the integrated water and fertilizer system is fertilization equipment or a fertigator which is usually installed at the head of the irrigation system. Its main function is to mix the irrigation water and fertilizer solution in a certain proportion and inject the mixture into the irrigation pipe network (Ayim et al., 2018). The commonly used fertigators mainly include: a pressure differential fertilizer tank, venturi fertigator and hydraulic proportional injection pump (Wang H.T. et al., 2018).

Fertigation systems offer precise control over the timing, quantity, concentration, and ratio of nutrients supplied to crops (Dadzie et al., 2013; Huang et al., 2009). This enhanced level of control results in greater yields and improved quality compared to traditional fertilization methods. Wang et al., (2018) noted that this contemporary agricultural technique is an effective way to optimize crop production while reducing environmental pollution. Fertigation can be implemented with any irrigation system, however, using an open irrigation system may result in uneven nutrient distribution across the field (Li S, 2020; Meng et al., 2007; Burt et al., 1995). Nevertheless, pressurized irrigation methods such as drip, sprinkler, and micro sprinkler systems are particularly well-suited for effective fertigation practices (Nagaraju et al., 2023; Zhao, 2023; Yuan et al., 2000).

Fertilizer application equipment comes in a variety of forms and types (Mao et al., 2023; Chen, 2022) that may have low fertilizer uniformity, unstable fertilizer application volumes, and incorrect fertilizer application volumes, resulting in a reduced effective fertilizer action during the growing cycle and burning of seedlings. Fertilization device is the core component of the fertilizer applicator, and its working performance determines the performance of the entire fertilizer applicator (Diyniyan, 2017; Geng et al., 2011). Different fertilizer application devices are selected according to different fertilizer application requirements, fertilizer types, and other factors (Liao, 2023; Chen, 2022; Wang, Q.L. et al., 2018). Hence, reasonable control of the fertilizer application volume and fertilizer uniformity becomes the key to solving the problem (Han et al., 2023; Liu, 2020).

Many scholars have conducted theoretical and experimental analyses of centrifugal fertigation equipment. Kweon and Grift (2006), Fulton et al., (2005) and Campbell et al., (2010) performed tests for a variable-rate fertigator with different structures and different control systems to determine the effect of these parameters on the performance of the applicator, as well as to establish the variation of fertilizer particle distribution under different influence factors. Hu C. et al., (2023) designed a pneumatic fertilization device and control system for paddy fields. The pneumatic conveying method is adopted to realize fertilizer conveying. Zhao et al., (2023) designed a stepped fertilization device. Through theoretical analysis and design calculation, the basic structural parameters of the guide curve of the ladder-fertilizing groove on the side of the subsoiling shovel were determined. Li et al., (2020) and Hu et al., (2020) researched the discharge pattern of the scraper-type fertilizer discharge device and determined the optimum values of scraper opening, scraper width, and forward speed. Li et al., (2020) conducted a design and kinematic analysis of the spiral churn to determine the structural parameters of the spiral churn and the range of parameter variations that affect the performance factors of the spiral churn unit. Chen (2023) designed a spiral push type lateral deep fertilization device and carried out an experimental analysis of the device performance. Li (2020) used a combination of theoretical analysis, simulation analysis, and bench test to improve the key components of the churn and chain rake intermediate conveying device and determined the structural and kinematic parameters of the key components of the conveying device.

With the sustainable development of precision agriculture and the steady progress of variable-rate fertilization technology, the proportional fertigator has attracted research attention due to its high efficiency combined with low cost and incidence of damage. The valve-regulated proportional fertigator was manufactured by Miracle-Gro in the United States. Compared with other fertigators, valve-regulated proportional fertigator has the advantages of small size, easy operation, low-starting pressure, constant and adjustable fertilizer concentration, no need for additional power, low-cost which is about 1/20 of the ordinary proportional fertilizer pump (Tayel et al., 2010; Bracey et al., 2003). Hence, the hydraulic performance of the valve regulated fertigator needs to be further studied due to current developments and practical application in engineering. In this paper, the operation mechanism, hydraulic performance and internal flow of the valve-regulated proportional fertigator were analyzed by means of the dynamic mesh simulation and verified by an experiment. This is important to address problems related to low fertilizer utilization and uneven distribution in the artificially drained catchments.

Materials and Methods

Structure and Operating Principle

The valve-regulated proportional fertigator uses the pressure of irrigation water to achieve fertilizer absorption without additional driving device. Figure 1 shows the basic structure of the fertigator. According to its function, the mechanical structure can be divided into three main parts: flow regulation, fertilizer extraction and fertilizer storage.

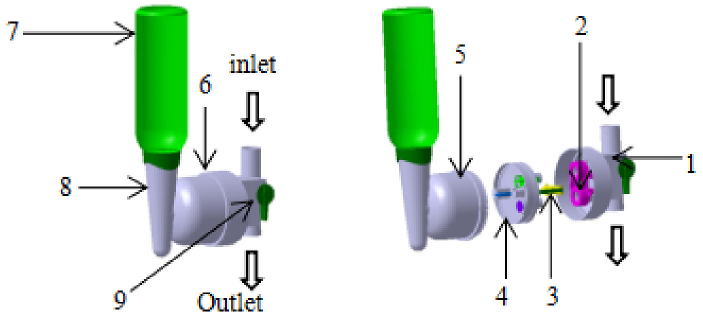

Valve Body, 2. Valve Core, 3. Piston Rod, 4. Driving Piston, 5. Sucker Piston, 6. Driving Chamber, 7. Fertilizer Storage, 8. Fertilizer Extraction, 9. Flow Regulation

Figure 1. Structure diagram of the valve-regulated fertigator

The valve-regulated proportional fertigator dispenses water through a three-way flow regulating valve. The diversion ratio of the three-way valve is achieved by varying the relative angle position between the valve core and the valve body. Water flows through the driving chamber of the fertigator for fertilizer extraction, and the water from the vertical outlet of the valve flows directly to the fertigator outlet and further combines with the water and fertilizer mixture in the fertilizer extraction part. Under the condition of constant inlet pressure and flow rate of the fertigator, the higher the horizontal diversion ratio, the higher the inlet flow rate at the fertilizer extracting end. The higher the piston movement frequency, the more the amount of fertilizer extraction, and the higher the fertilizer application ratio.

The fertigator uses the pressure of the irrigation water to make the driving piston produce the pressure difference between the left and the right sides to make it move. The piston rod and the sucker piston fixed in the driving piston are driven by the pressure difference to move together with the driving piston in the barrel. On the right stroke, the water from the horizontal outlet of the diversion three-way valve enters the left cavity of the driving piston, pushes the driving piston to move to the right, and expels the liquid from the right cavity of the driving piston. The fertilizer piston moves to the right with the driving piston, and the fertilizer liquid is pumped from the fertilizer liquid bottle to the fertilizer suction cylinder. At the end of the right stroke, under the action of the reversing mechanism, the change in the opening and closing of the reversing valve changes to the left stroke. The water from the horizontal outlet of the diversion three-way valve enters the right cavity of the driving piston during the left stroke and drives the driving piston to move to the left. At the same time, the liquid from the left cavity of the driving piston is discharged. At the end of the left stroke, under the action of the reversing mechanism, the opening and closing situation of the reversing valve changes, switching to the right stroke, repeatedly.

Numerical Calculation

Figure 2 shows a schematic diagram of the internal structure of the fertilizer applicator. In order to show the internal flow more conveniently, the reversing valve port on the driving piston was rotated into the plane, where the inlet pipe and the outlet pipe are located. From the right stroke as illustrated in Fig. 2(b), water flows from the horizontal outlet of the three-way valve into the left cavity, causing the piston to shift to the right and expel the liquid. The piston advances to the right alongside the driving piston to transfer the liquid to the fertilizer suction cylinder. The alteration in the operation of the reversing valve results in a transition to the left stroke. During this left stroke, water from the horizontal outlet of the three-way valve enters the right cavity of the driving piston, propelling the piston to move left as can be seen in Fig. 2(a). Concurrently, the liquid from the left cavity of the driving piston is expelled, and the operation of the reversing valve continues to change, repeatedly alternating back to the right stroke. The angle (α) of the three-way valve is the angle between the centerline of the vertical outlet and the valve core.

Due to the limitation of the existing dynamic mesh technology, it was impossible to simulate the driving piston and the fertilizer piston simultaneously. At the same time, when designing the simulation scheme of the driving part, the internal reversing mechanism was initially removed, and the piston motion process was divided into two stages: left stroke and right stroke. In addition, because the structure of the driving piston and the inlet and outlet pipes is too complex and the calculation domain was irregular, it is difficult to realize it by using the moving grid technology. Therefore, the inner flow passage of the driving piston part of the fertilizer applicator, shown in Fig. 2, was simplified, and the simplified flow mechanism of the driving part after retaining the main hydraulic parameters is shown in Fig.3. For the convenience of viewing the post-processing pictures, the gap between the left and right cavities indicates the piston and wall thickness, in which the driving piston diameter (*D)* = 72 mm, driving piston stroke *(L)* = 29 mm, inlet and outlet diameter *(d)* = 13.2 mm.

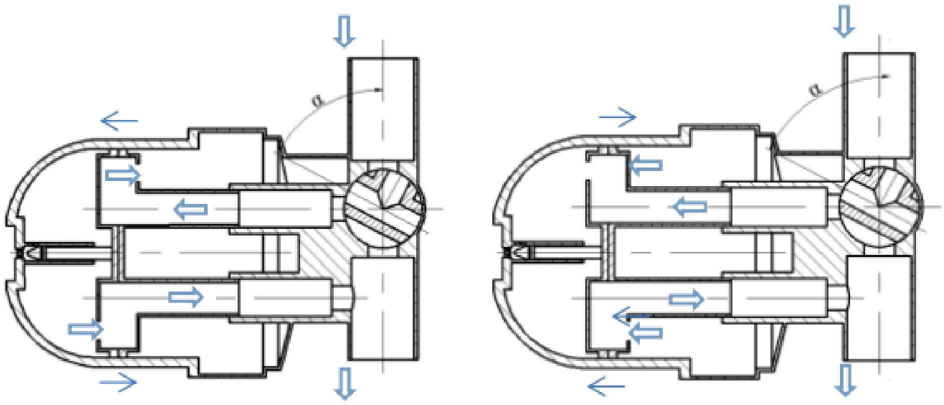

(a) Left stroke (b) Right stroke

Figure 2. Internal flow mechanism of the valve-regulated fertigator

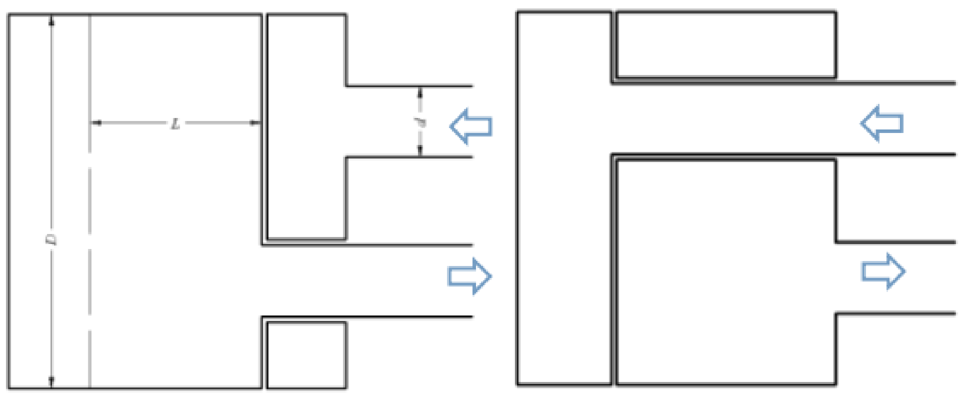

(a) Left stroke stage (b) Right stroke stage

Figure 3. Streamline simplification of the valve-regulated fertigator

At the same time, when designing the simulation scheme of the driving part, the internal reversing mechanism was initially removed, and the piston motion process was divided into two stages: left stroke and right stroke. In addition, because the structure of the driving piston and the inlet and outlet pipes is too complex and the calculation domain was irregular, it is difficult to realize it by using the moving grid technology.

Mesh generation and updating

The hydraulic performance and internal flow of the fertigator were numerically simulated by using the dynamic grid technology in Fluent software. In this paper, the hexahedron structure grid was used in the calculation domain of the fertilizer extracting part of the fertigator as shown in Fig. 4. Hence, the dynamic stratification model was selected, and the splitting factor was 0.4, while the contraction factor was 0.04.

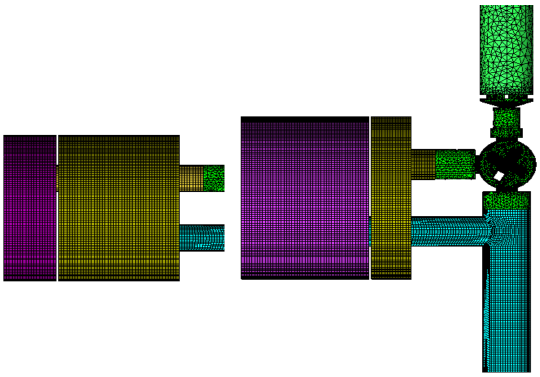

Figure 4. Meshed water body in the valve-regulated proportional fertigator

Taking the fertigator with the angle of 60° of the three-way valve as an example, the water grid of the final left-way stage was 1044751, and the water grid of the three-way valve was 644229, the water grid of the right-hand cavity was 78629. In addition, the water grid of the left-hand cavity was 235270, the water grid of the outlet was 86623, and the water grid of the right-hand stage was 1037913, of which the water grid of the right-hand stage was 78629. The grid number of the cavity water was 199894, the grid number of the left cavity water was 96199, the grid number of the outlet water was 80959, and the grid number of inlet water was 16632.

Experimental verification

The schematic diagram of the test stand is shown in Fig. 5. A certain amount of water was stored in the storage tank 1, and the pressure water drawn from the pump 2 enters the main pipe. Ball valve 3 was installed on the main pipe (PVC pipe) to regulate the inlet flow and pressure. The experiments were conducted in accordance with the ISO5690-2-1984 and ASAE S341.2 protocols.

A flow meter 4 with 0.5% accuracy and an intelligent turbine flow meter LWGYE-40) was used to monitor the inlet flow of the fertigator. Pressure gauges 5 and 6 (2.5 accuracy) were installed at the inlet and outlet of the fertigator to measure the inlet and outlet pressures. The pressure difference between the inlet and outlet fertilizer applicator (because the outlet is directly connected with the atmosphere) of the fertilizer applicator was varied by adjusting the ball valve, and the pressure difference was taken as the inlet pressure. Meanwhile, the fertilization ratio was changed by adjusting the handle angle of the three-way flow control valve of the fertilizer applicator. The measured inlet pressure was 0.14 MPa, and all valve angles were 0, 5, 10, 15, 20, 25, 30, 35, 40, 45, 50, 55, 60, 65, 70, 75, 80, 85, and 90°.

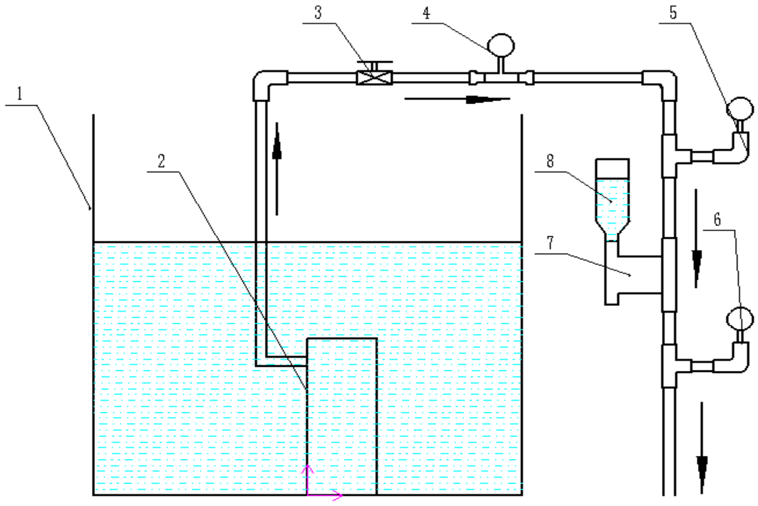

1. Storage Cylinder, 2. Pump, 3. Ball Valve, 4. Flowmeter, 5, 6. Pressure Gauge,
7. Valve Adjustable Proportional Fertilizer, 8. Fertilizer Liquid Bottle

Figure 5. Hydraulic performance test bench for the valve-regulated fertigator

The actual operation measurement of hydraulic performance test was done as follows: first, the three-way valve was adjusted to 0° position. The ball valve in the inlet pipeline was opened before the introduction of a fertilizer. The inlet ball valve was rotated after running the pump in a stable pressure meter reading of 0.14 MPa, the flowrate was read and recorded. The key data of mouth flow, fertilizer amount and piston motion frequency were analyzed and discussed.

Results and Discussion

Internal Flow Analysis

Figure 6 shows the variations of flow velocity on the Y-Z plane in the left and right phases of the fertigator when the three-way valve angle was 70° degrees and the inlet pressure was 0.14 MPa. From the diagram, the highest flow velocity area in the fertigator was concentrated in the inlet one-way and three-way valve. The maximum flow velocity was 13 $m \cdot s^{-1}$, while the fertilizer extraction part and the outlet part were in the low flow velocity area. The flow area of the one-way and three-way valve part shrinks rapidly, thus making the three-way valve divide horizontally at 70° degrees. Most of the water flows from the horizontal outlet of the valve to the driving chamber, so the velocity of the driving chamber near the horizontal outlet of the valve was relatively large. The driving chamber and the outlet chamber on both sides of the piston were much larger than other parts, hence the velocity of the flow was very low, and the kinetic energy was converted into pressure energy to drive the movement of the piston. The liquid from the outlet cavity entered the horizontal outlet section, and because the flow area was small, the flow velocity increased slightly, but the flow area increased and decreased after entering the outlet section of the fertigator.

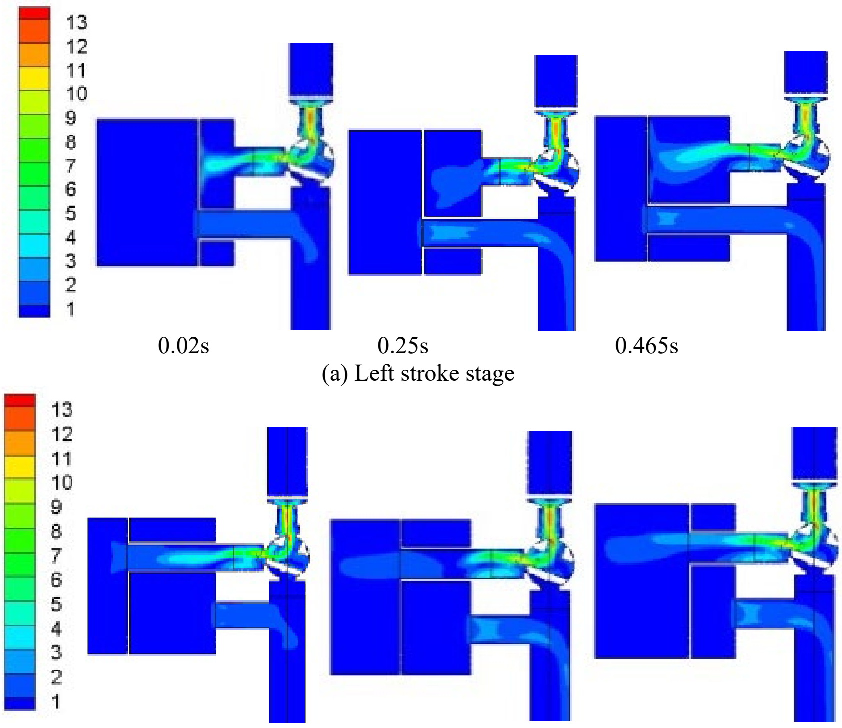

Figure 6. Velocity cloud map (unit: m·s^{-1})

Figure 7 shows that the piston was driven by the water flow in the driving chamber, and the part of the pressure energy was transformed into mechanical energy of the piston, because the pressure in the chamber was small. The liquid in the outlet chamber was gradually discharged under the action of the piston, and the region remained in a low pressure state; the junction of the horizontal outlet of the three-way valve and the inlet of the driving chamber, the horizontal outlet of the chamber and the outlet of the fertilizer applicator, and the left stroke were near the end at the rapid expansion of the section. When the point is far away from the near wall of the piston, the fluid particle has inertia, and the fluid cannot rapidly bend and expand according to the pipe shape, hence the fluid and the pipe wall at the corner of the pipe break off to form a vortex zone, resulting in the energy loss. The pressure in these areas was lower than the surrounding area and the fertilizer used pressure from the water to drive the piston movement to achieve pumping.

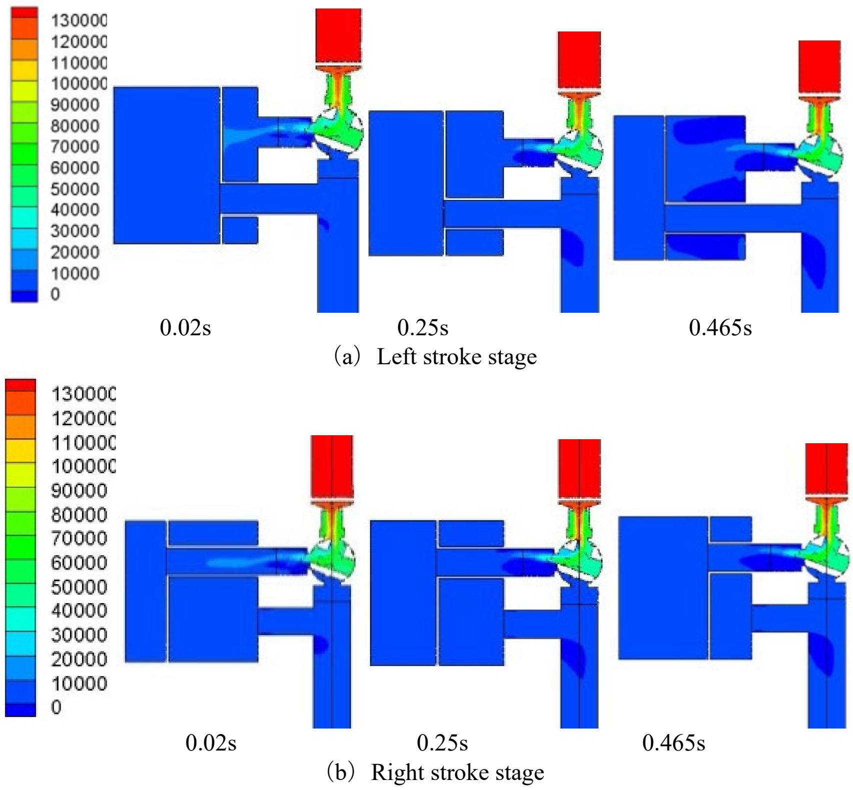

Figure 7. Pressure cloud map (unit: Pa)

Force and motion analysis of piston

The relationship between the force acting on the right side of the piston during the left stroke and the drag acting on the left side is illustrated in Fig. 8. On the contrary, the resultant force acting on the piston during the right stroke was the difference between the driving force and the drag. It can be seen from the diagram that the driving force was much greater than the resistance at the beginning of the piston movement, hence the resultant force curve of the piston almost coincides with the driving force curve; the driving force and the resistance fluctuate from the initial maximum value to the same stable value based on this value, accordingly, the resultant force of the piston was also sharply reduced from the initial maximum of 242 MPa value to 0 and then attached to this value. Fluctuating near and below.

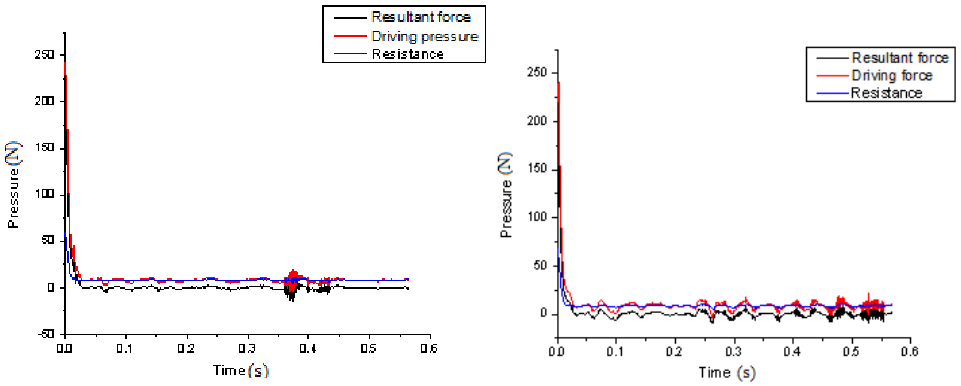

(a) Left stroke stage (b) Right stroke stage

Figure 8. Force and motion of piston

Specifically, starting from the left stroke, the maximum driving force was 221 N, the maximum resistance was 69 N, and the resultant force of the piston was 152 N. At about 0.015 s, the resultant force of the piston first decreased to approximately 8.5 N, then fluctuated up and down. At about 0.03 s, the resultant force of the piston decreased to about 8.5 N, the resultant force of the piston became 0, and the piston movement reached a stable state and continous. At the beginning of the right stroke, the maximum driving force was 242 N, the maximum resistance was 60 N, and the resultant force of the piston was 182 N. At about 0.015 s, the resultant force of the piston decreased to about 8.5 N, then fluctuated up and down, and at about 0.03 s, the driving force decreased to about 8.5 N. When the resultant force of the piston approaches zero (0) and the force of the piston achieves steady state and always fluctuates slightly in this state. It is more likely that the resultant force is near zero and fluctuating, or the 8.5 N value is the driving force, and the resultant force is the difference between the driving force and the damping force. This finding is consistent with Zhang et al., (2024) who observed that as the rotational speed increases, the coefficient of variation of the axial distribution of the force chains gradually decreases. Meanwhile, the uniformity of the circumferential distribution of the force initially increases and then decreases.

Comparison between simulation and experimental results

As can be seen in Fig.9, the simulated inlet flow rate curve of the valve - regulated proportional fertilizer applicator was compared with the experimental curve. It can be seen from the graph that the two curves have the same trend, both are V-shaped and opening upward, and the curves after 45^{o} were slightly smaller compared with those before 45^{o} degrees.

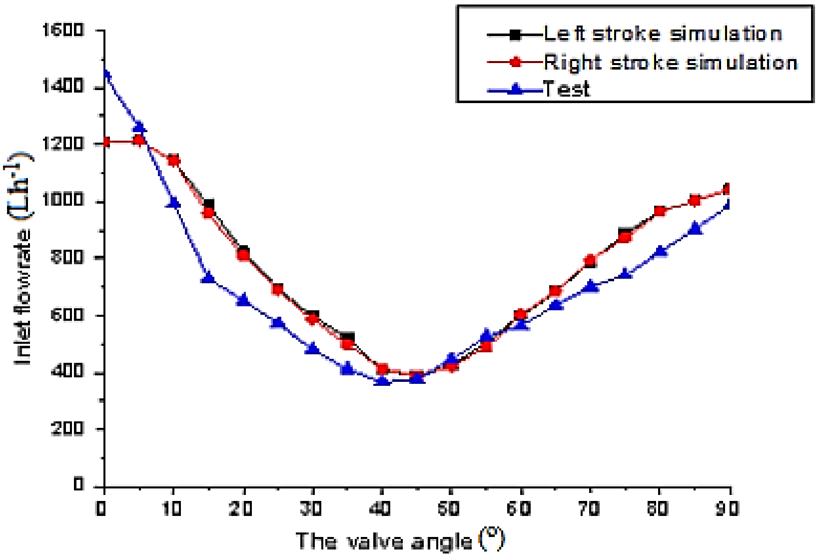

Figure 9. Comparison of experimental and simulated angle-flow curves

This was mainly caused by the increase in the resistance coefficient of the fertigator during the fertilizer extraction process. The error between simulation and test was slightly larger with the maximum relative error of 15%. However, there was no difference in the overall trend, so we can draw a reasonable and accurate conclusion of the simulation. The obtained result was consistent with the study of Ferrari et al., (2018) who observed similar trends with both exhibiting a v-shape that opens upward, indicating flow rate increases with certain operational parameters, though the curves after 45° were noted to be slightly smaller than before.

Conclusions

1. The area with the highest flow velocity of 13 $m \cdot s^{-1}$ in the fertigator concentrates on the inlet one-way valve and three-way valve part, while the fertilizer extraction part and the outlet part were in the low flow velocity area. The total pressure of the fertigator inlet was much higher due to the local resistance loss, the pressure was low at the sudden expansion of the section.
2. At the initial stage of piston motion, the driving force was much greater than the resistance, and the driving force and the resistance fluctuated from the initial maximum to the same stable value. The resultant force of piston fluctuates from the initial maximum driving force of 242 N to 0 N, and then the piston accelerated from 0 N to the minimum driving force of 8.5 N. When the resultant force was reduced, the acceleration was also

decreased. However, when the acceleration was reduced to zero (0), the piston started to move uniformly.

3. The maximum relative error between simulation and experiment 15%. However, there was no difference in the overall trend, so we can draw a reasonable and accurate conclusion of the simulation.
4. The obtained results can be a prerequisite for achieving uniformity in the spread of fertilizer application in the artificially drained catchment.

Author Contributions: Zakaria Issaka is the Sole Author

Conflicts of Interest: The author declare no conflict of interest in this paper.

Funding: This research received no external funding.

Acknowledgments: I express my sincere gratitude to Dr. Wilson Mwanga who contributed to proofreading this paper and successful completion of this study.

References

ASAE (1994). S341.2: Procedure for measuring distribution uniform and calibrating granular broadcast spreaders. *Applied Engineering in Agriculture, 10*(6), 783-786.

Ayim, I., Ma, H.L. & Alenyorege, E.A. (2018). Optimizing and predicting degree of hydrolysis of ultrasound assisted sodium hydroxide extraction of protein from tea (*Camellia sinensis* L.) residue using response surface methodology. *Journal of Food Science Technology,* 55, 5166-5174.

Bracey, R.P., Parish, R.L. & Rosendale, R.M. (2003). Fertigation uniformity affected by injector type. *HortTechnology,* 13, 103-105.

Burt, C.M., O'Connor, K. & Ruehr, T. (1995). Fertigation. Calif. Irrigation Research and Training Center, California Polytechnic University, California, USA.

Campbell, C.M., Fulton, J.P, Mcdonald, T.P, Wood, C.W, Zech, W.C. &Srivastava, P. (2010). Spinner-disc technology to enhance the application of poultry litter. *Applied Engineering in Agriculture*, 26(5): 759-767.

Chen, A. (2022). The development status of organic fertilizer and its supporting fertilizer application machinery. *Agricultural Machanization*, 9, 1-5.

Chen, C. (2022). Design of spiral pushing lateral deep fertilization device synchronized with rice transplanting. *Journal of Agricultural Mechanization Research,* 45, 71-75.

Dadzie, R.G., Ma, H.L., Abano, E.E., Qu, W.J. & Mao, S.Y. (2013). Optimization of process conditions for production of angiotensin I-converting enzyme (ACE) inhibitory peptides from vital wheat gluten using response surface methodology. *Food Science Biotechnology,* 22, 1531-1537.

Daniyan, I.A. (2017). Development and performance evaluation of organic fertilizer machinery. *Cogent Engineering,* 4, 1364044.

Ferrari, A., Pizzo, P. & Rundo, M. (2018). Modelling and experimental studies on a proportional valve using an innovative dynamic flow-rate measurement in fluid power system..*Journal of Mechanical Engineering Science,* 232, 42-68.

Fulton, J.P., Shearer, S.A., Higgins, S.F., Hancock, D.W. & Stombaugh, T.S. (2005). Distribution pattern variability of granular VRT applicators. *Transactions of the American Society of Agricultural Engineering,* 48(6),2053-2064.

Geng, D., Zhang, D. & Wang, X. (2011). *New Edition of Agricultural Mechanics*; National Defense Industry Press: Beijing, China; Volume 12.

Han, W., Sun, J., Zhang K., Mao L., Gao L., Xuemin Hou, X., Cui N., Kang, W. & Gong, D. (2023).Optimizing drip fertigation management based on yield, quality, water and fertilizer use efficiency of wine grape in North China. *Agricultural Water Management*, 280, 108188.

Hu, C. (2022). Design and test of pneumatic fertilizer apparatus in paddy field. *Journal of China Agricultural Mechanization,* 43, 14-19.
Hu, J., Wang, Y. & Wu, Y. (2020). Design of inclined scraper type solid organic fertilizer applicator. *Journal of Agricultural Mechanization Research,* 42, 121-124.
Huang, X., Li, G. & Wang, M. (2009). CFD simulation to the flow field of Venturi injector. *International Federation for Information Processing,* 294(2), 805-815.
ISO5690-2-1984: Equipment for distributing fertilizers-test methods-Part 2: Fertilizer distributors in lines.
Kweon, G. & Grift, T.E. (2006) Feed gate adaptation of a spinner spreader for uniformity control. *Biosystems Engineering,* 95(1), 19-34.
Li, E. (2020). Design and Testing of a spiral churn-type water field strip tillage and fertilizer mixing device. Ph.D. Thesis, Tohoku University of Agriculture, Sendai, Japan.
Li, J.S., Du, Z. & Li, Y. (2008). Field evaluation of fertigation uniformity for subsurface drip irrigation systems. *Transaction of China Society of Agricultural Engineering,* 24, 83-87.
Li, L., Zhang, Y. & Liao, Y. (2022). Research on the law of fertilizer discharge of scraper type fertilizer discharge device. *Journal of Agricultural Mechanization. Research,* 44, 149-152.
Li, S. (2020). Design and test of key components of oil sunflower combine harvester intermediate conveyors. Huazhong Agricultural University, Wuhan, China.
Liao, Q. (2023). Design and Experiment of Side Deep Hole Fertilization Device for Rapeseed. *Transaction of China Society of Agricultural Machanization, 54*, 41-52.
Liu, J.S. (2020). Numerical simulation of Fertilizer Shunt-Plate with uniformity based on EDEM software. *Computer Electronic Agriculture*, *178*, 105737.
Meng, Y., Li, J. & Li, W. (2007). Experimental study on fertilization performance of differential pressure fertilization tank in micro-irrigation system. *Transactions of the Chinese Society of Agricultural Engineering,* 23(3), 41-45.
Nagaraju, V. K., Nagarajan, K., Kannan, B., Ramanathan, S., & Duraisamy, R. (2023). Numerical simulation of soil water dynamics in automated drip irrigated Okra field under plastic mulch. *Agricultural Engineering*, *27*(1), 11-32.
Tayel, M.Y., Eldardiry, E.I. & Shaaban, S.M. (2010). Sabreen, K.P. Effect of injector types and irrigation and nitrogen levels on, III-cost analysis of garlic production. *Journal of Applied Science Research,* 6, 822-829.
Wang, H.T., Chen, Y.Y., Wang, J.D., Yang, B., Mo, Y. (2018). Experimental study on comprehensive working performance of Venturi injector. *Journal of Drainage, Irrigation and Machanization Engineering,* 36, 340-346.
Wang, Q.L., Wang, Z.H., Wu, W.Y. & Liao, R.K. (2018). Throat structure optimization and flow field analysis of ATP Venturi fertilizer applicators. *Journal of Drainage, Irrigation and Mechanization Engineering,* 36, 829-834.
Yuan, Z., Choi, C.Y. & Waller P.M. (2000). Effects of liquid temperature and viscosity on venture injectors. *Transactions of the American Society of Agricultural Engineering,* 43(6), 1441-1 447.
Zhang, M., Niu, H., Han, Y., Zhi, Y., Yuan, T., Zhang, H., He, Y., Tang, Z. & Lan, H. A. (2024). Simulation and experiment of the flow fluctuation characteristics of a fertilizer distribution apparatus with a screw from the perspective of the force chain. *Applied Science,* 2024, *14*, 1122.
Zhao, Y. (2011). Development of hydrodynamic proportional fertilizer pump. *Modern Agricultural Equipment,* 8, 48-50.
Zhao, Y. (2023). Design and analysis of step fertilization device based on tillage and sowing machine. *China South Agricultural Mechanization,* 54, 1-4.

SYMULACJA DYNAMICZNA I WALIDACJA EKSPERYMENTALNA WYDAJNOŚCI HYDRAULICZNEJ DLA FERTYGATORA PROPORCJONALNEGO REGULOWANEGO ZAWOREM

Streszczenie. Wraz ze zrównoważonym rozwojem rolnictwa precyzyjnego, regulowany zaworem proporcjonalny fertygator przyciągnął uwagę badaczy ze względu na wysoką wydajność połączoną z niskimi kosztami i częstością występowania uszkodzeń. Aby zbadać wydajność hydrauliczną fertygatora, przeprowadzono analizę przepływu wewnętrznego, siły i ruchu tłoka za pomocą symulacji dynamicznej i walidacji eksperymentalnej. Wyniki pokazują, że przepływ wlotowy nawozu najpierw wzrósł, a następnie zmniejszył się wraz ze wzrostem kąta otwarcia zaworu trójdrożnego przy tych samych warunkach ciśnienia. Obszar o najwyższej prędkości przepływu wynoszącej 13 m/s w fertygatorze koncentruje się w części wlotowej zaworu jedno i trójdrożnego, podczas gdy część ekstrakcyjna nawozu i część wylotowa znajdują się w obszarze o najniższej prędkości przepływu. Częstotliwość ruchów wzrastała wraz ze wzrostem kąta zaworu trójdrożnego, z wyjątkiem części środkowej, w której zaobserwowano zmiany w zmianie fali. Wraz ze wzrostem ciśnienia wlotowego rosły również wahania kątów otwarcia zaworów trójdrożnych. W początkowej fazie ruchu tłoka siła napędowa była znacznie większa niż opór, a siła napędowa i opór wahały się od początkowego maksimum do tej samej, stabilnej wartości. Wypadkowa siła tłoka zmienia się od początkowej maksymalnej siły napędowej wynoszącej 242 N do 0 N, a następnie tłok przyspiesza od 0 N do minimalnej siły napędowej wynoszącej 8,5 N. Gdy wypadkowa siła została zmniejszona, przyspieszenie również uległo zmniejszeniu. Jednakże, gdy przyspieszenie spadło do zera (0), tłok zaczął poruszać się równomiernie, co jest przydatne do osiągnięcia równomiernego rozprowadzania nawozów w sztucznie odwodnionej zlewni. Maksymalny błąd względny między symulacją a eksperymentem wyniósł 15%. Nie zaobserwowano jednak różnicy w ogólnym trendzie, co pozwala na wyciągnięcie racjonalnych i dokładnych wniosków z symulacji. Badanie może być przydatne do osiągnięcia równomiernego rozprowadzania nawozów w sztucznie odwodnionej zlewni.

Słowa kluczowe: Proporcjonalny fertygator regulowany zaworem, trójdrożny zawór sterujący przepływem, stosunek nawozu, dynamiczna siatka, siła napędowa